Standardizing thermal contrast among local climate zones at a continental scale

Xuan Chen[1], Jiachuan Yang[1, *], Chao Ren[2], Sujong Jeong[3], Yuan Shi[4]

[1]Department of Civil and Environmental Engineering, The Hong Kong University of Science and Technology, Hong Kong, China

[2]Faculty of Architecture, The University of Hong Kong, Hong Kong, China

[3]Department of Environmental Planning, Graduate School of Environmental Studies, Seoul National University, Seoul, South Korea

[4]Institute of Future Cities, The Chinese University of Hong Kong, Hong Kong, China

Corresponding author: Jiachuan Yang (cejcyang@ust.hk)

Key Points:

- Observed temperatures over different local climate zones change with geographical conditions across China
- Characteristic temperature regimes of local climate zones are consistent at the continental scale after removing the effect of geographical conditions
- Annual mean standard thermal contrast for studied local climate zones is 0.51 ℃ at night and 0.22 ℃ during daytime.

Abstract

The Local Climate Zone (LCZ) system provides a standardized framework for intra-urban heat island studies. Yet the thermal contrast of air temperatures over different LCZs has not been examined at a large scale. Using ground-based meteorological observations in 2016, here we investigated the thermal behaviors of various LCZs over China. Measured temperatures over studied LCZs are found to have strong relations with latitude, altitude, and the distance to coastline. Thermal contrasts reduce to less than 1 ℃ in all seasons after removing the signal of background mean temperature determined by geographical conditions. The warmth of urban LCZs is more evident at night, with an annual mean temperature difference of 0.51 ℃ compared to the low-plant rural LCZ. Despite the temperature variation within individual LCZs, derived standard thermal contrasts are insensitive to changes in geographical conditions. Results reveal that consistent characteristic temperature regimes of LCZs exist at the continental scale.

Plain Language Summary

The local urban landscape has essential impacts on air temperatures above it, whether such impacts are consistent in different cities remains unclear in the literature. We used temperature data from meteorological stations to investigate the thermal behaviors of urban neighborhoods with distinct landscape properties over China. At the continental scale, air temperatures correlate strongly with geographical conditions including latitude, altitude and the distance to coastline. After removing the effect of geographical conditions, the impact of local urban landscape on air temperature is found to be consistent though with considerable variations. The warmth of urban neighborhood is more evident at night compared to during daytime. Estimated temperature differences among different urban neighborhoods and a reference rural area are generalizable for other cities in China. This study demonstrates the relation between local landscape and urban microclimate, and can provide guidance for urban planning with regards to the outdoor thermal environment.

1 Introduction

Land use/land cover conditions have significant impacts on local and regional meteorological variables. One of the most evident examples is the Urban Heat Island (UHI) effect, where urbanization leads to higher temperatures in cities compared to their surrounding countryside (Oke, 1982). Elevated temperatures in cities have adverse impacts on building energy consumption and public health during hot periods (Santamouris et al., 2015; Tomlinson et al., 2011), and past decades have seen increasing UHI studies around the world (Barreca et al., 2016; Chen & Jeong, 2018; Levermore et al., 2018; Zhou et al., 2017). The widely-used UHI intensity, defined as the urban-rural temperature difference, is nevertheless sensitive to the selection of ‘urban’ and ‘rural’ sites (Martilli et al., 2020). With dense meteorological networks deployed in recent years, high-resolution observations reveal that the intra-urban climate variability between neighborhoods can be as large as the urban-rural difference (Ramamurthy et al., 2017; Yang & Bou-Zeid, 2019). To better link local climate with landscape properties, Stewart and Oke (2012) developed the Local Climate Zone (LCZ) system that included ten built types and seven land cover types. Each LCZ type has distinguished features of surface cover, structure, material, and human activities, and has a unique characteristic air temperature regime that is most pronounced on dry, calm and clear nights (Stewart & Oke, 2012).

The LCZ system provides an objective framework for local-scale temperature studies in different cities. Studies have adopted the LCZ scheme with in-situ measurements to assess the intra-urban temperature variability in major metropolitan areas, including Hong Kong, Vancouver, Nagona, Uppsala, Berlin and Phoenix (Fenner et al., 2017; Stewart et al., 2014; Wang et al., 2018; Zheng et al., 2018). Reported thermal contrasts among various LCZs in studied cities evaluated the validity of the LCZ classification system, yet the analysis of air temperature was mostly conducted at the city scale and for a short study period. For example, Alexander and Mills (2014) studied the relationship between air temperature and LCZ in Dublin for one week. It is worth mentioning that surface temperature differences among LCZs have been investigated for 50 cities using satellite data (Bechtel et al., 2019). However, air temperature is of paramount interest for urban climate studies given its implications for outdoor thermal comfort and building energy consumption. Though one primary aim of the LCZ system is to standardize cross-city comparisons, air temperature contrasts among different LCZs have not been studied at a large scale.

Over a large spatial extent, geographical condition and atmospheric forcing vary significantly and play important roles in regulating meteorological variables. Wienert and Kuttler (2005) found the dependence of urban-rural temperature difference on latitude and suggested a larger maximum UHI intensity in high-latitude regions. Thermal contrasts among different LCZs can therefore change from city to city as local landscape only contributes partially to determining the air temperature. For example, annual mean nocturnal air temperature of LCZ 5 is about 4.4 °C higher than that of LCZ D for ideal days in Szeged, Hungary (Skarbit et al., 2017), but the difference is less than 1 °C in Nanjing, China (Yang et al., 2018). The question then becomes whether the inconsistent thermal contrast between these two LCZs is caused by the difference in geographical and climatic conditions. Following the concept of the LCZ scheme, the impact of local landscape on air temperature needs to be distinguished from those of background climate and environment. This can only be achieved through large-scale analysis because geographical and climatic conditions are nearly identical at the city scale.

How does the characteristic temperature regime of LCZs change with geographical and climatic conditions? Is there a consistent thermal contrast among different LCZs at a large scale? How large is the temperature variability of individual LCZs compared to their thermal contrast? Answers to these questions can advance our understanding of the relation between local landscape and air temperature. To that end, we combine ground-based meteorological measurements and LCZ map to conduct a continental-scale comparative analysis over China.

2 Materials and Methods

2.1 Air temperature measurement

Hourly air temperature data measured at 2 m height above the ground level from 2131 meteorological stations was collected from the National Meteorological Information Center of the China Meteorological Administration. For consistency with the LCZ map, the study period is one full year of 2016. We defined seasons as follows, spring: March - May, summer: June - August, fall: September - November, and winter: December - February. To look into thermal contrasts during the diurnal cycle, we defined daytime as 0900 - 1500 local time and nighttime as 2100 - 0300 local time.

105 2.2 Classification of meteorological stations

106 In this study, we utilized the 2016 LCZ map of China developed using an improved
107 method of the World Urban Database and Portal Tool (WUDAPT). Accuracy of the LCZ
108 classification method has been extensively evaluated for various Chinese cities (Cai et al., 2018;
109 Shi et al., 2018). The LCZ map has a spatial resolution of 100 m × 100 m and includes 10 built
110 types (urban LCZs) and 7 land cover types. Locations of meteorological stations were overlaid
111 with the LCZ map to classify the air temperature measurements into different LCZ types.
112 Landscape homogeneity was checked to ensure measured data can represent characteristic
113 temperature regimes of different LCZ types. As the minimum radius to define LCZs is 200 -
114 500 m (Stewart & Oke, 2012), we estimated the dominant LCZ types within 3 × 3 grids and 5 ×
115 5 grids around each station. Only stations with matched dominant LCZ types were considered in
116 this study. For comparing temperature characteristics of LCZs at the continental scale, we
117 excluded the LCZ types with insufficient number of stations (< 40) or spatial span over China.
118 As a result, five urban LCZs (2: Compact mid-rise; 3: Compact low-rise; 4: Open high-rise; 8:
119 Large low-rise; 10: Heavy industry) and one rural LCZ (D: Low plants) were selected. To avoid
120 bias introduced by a small number of stations with distinct geographical conditions, we focused
121 on the area between 22° N – 40° N where the majority of urban LCZ stations fall (Fig. 1a). In the
122 end, a total of 745 stations were retained for analyses. The number of stations for each LCZ type
123 is shown in Fig. 1b, and the spatial distribution of studied stations is shown in Fig. 1c.

124

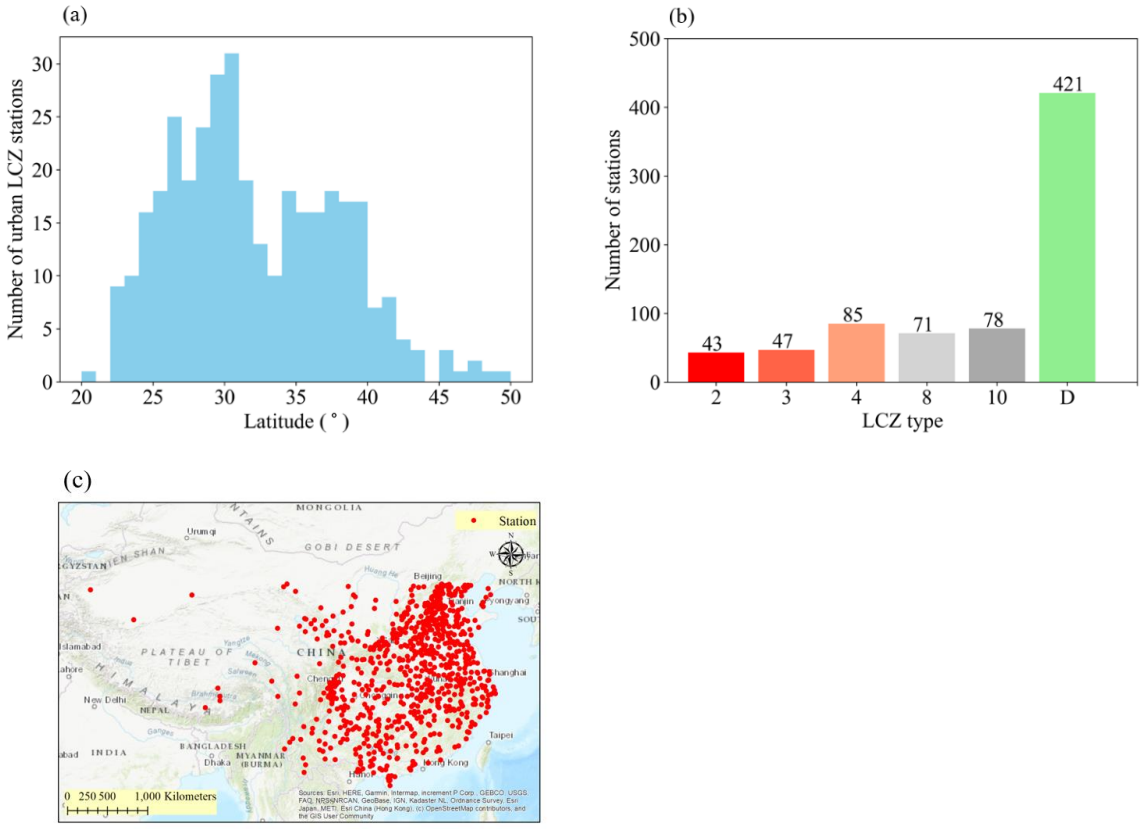

125

126 **Figure 1.** Distribution of meteorological stations over China. (a) Latitude distribution of urban
127 LCZ stations; (b) The number of stations in analyzed LCZ types in this study; (c) Spatial

distribution of studied stations over China. Land use types of LCZs: 2-Compact mid-rise, 3-Compact low-rise, 4-Open high-rise, 8-Large low-rise, 10-Heavy industry, D-Low plants.

2.3 Multiple linear regression

To estimate thermal contrasts among different LCZs at the continental scale, the dependence of air temperature on geographical conditions must be removed. Latitude (LAT), altitude (ALT) and the distance to coastline (DCL) are three critical parameters affecting the background mean temperature (Linacre & Geerts, 1997). An ordinary least squares regression analysis is then performed using these three parameters as independent variables and air temperature as the dependent variable to establish a multiple regression model of the best fit. The model is formulated as:

$$T_{pre} = \alpha_1 LAT + \alpha_2 ALT + \alpha_3 DCL + \beta + \varepsilon, \quad (1)$$

where T_{pre} is the predicted background mean temperature; α_1, α_2, and α_3 are the coefficients for LAT, ALT, and DCL respectively; β is the intercept; and ε is the residual

2.4 Raw and standard themal contrast

To highlight the thermal contrast among various urban neighborhoods and the rural area, we set the rural LCZ (type D) as the reference and compute the air temperature difference between urban LCZs (T_{ULCZ}) and it:

$$\Delta T_r = \sum(T_{ULCZ} - T_D), \quad (2)$$

where T_{ULCZ} and T_D are the measured temperature at individual stations belong to urban LCZs and LCZ D. We define ΔT_r as the raw thermal contrast, which has been employed in previous LCZ studies (Kotharkar & Bagade, 2018; Shi et al., 2018; Verdonck et al., 2018). Note that ΔT_r does not reveal the 'true' thermal contrast among different LCZs, as observed temperatures contain the signal of background mean temperature, which is determined by geographical conditions of stations.

Using the regression model detailed in section 2.3, we can remove the effect of geographical conditions on raw thermal contrast. The impact of local landscapes can be estimated as the deviation of measured temperature from the predicted background mean temperature. The deviation ΔT for each station is given by:

$$\Delta T = T_{obs} - T_{pre}\,(LAT, ALT, DCL), \quad (3)$$

where T_{obs} is the observed temperature, and T_{pre} is the predicted background mean temperature from regression models that corresponds to the geographical condition of each station.

Averaging ΔT for all stations of one LCZ class yields the characteristic temperature regime of the LCZ with respect to the background temperature. The standard thermal contrast (ΔT_s) independent of geographical conditions can be computed using LCZ D as the reference type:

$$\Delta T_s = \sum_{nULCZ}(T_{ULCZ} - T_{pre}) - \sum_{nD}(T_D - T_{pre}), \quad (4)$$

where nULCZ and nD denote the number of stations for each urban LCZ type and LCZ D, respectively. Note that two T_{pre} terms on the right-hand-side of Eq. (3) will not cancel out as the geographical condition of stations varies with LCZ types.

3 Results and Discussion

3.1 Raw thermal contrast among LCZs

The monthly variation of daily mean temperature for studied LCZ types is shown in Fig. 2a. Mean temperature of all LCZs is about 26.56 °C in summer and 5.59 °C in winter. The temperature variability among studied LCZs is the smallest in summer and the largest during winter. LCZ 2 has the highest temperature throughout the year while LCZ D has the lowest temperature. At the annual scale, the daily mean raw thermal contrast (ΔT_r) is 1.84 ± 0.46 ℃ (mean ± standard deviation among studied urban LCZs). Seasonal mean ΔT_r are shown in Fig. 2. Nighttime thermal contrasts (Fig. 2d) are found to be larger than daytime contrasts (Fig. 2c). Summertime daily mean ΔT_r are lower than 2 ℃ over all LCZs, while wintertime daily mean ΔT_r can reach up to 4 ℃ over LCZs 2 and 10 (Fig. 2b). Among the studied LCZs, compact mid-rise (LCZ 2) and heavy industry (LCZ 10) zones have the largest ΔT_r and large low-rise landscape (LCZ 8) has the smallest ΔT_r. The diurnal and seasonal variations of thermal contrasts here are consistent with previous studies, where urban-rural temperature differences found to be more evident in winter and during nighttime (Skarbit et al., 2017; Zhou et al., 2014). Nevertheless, results in Fig. 2 are biased by the unequal geographical conditions of stations in different LCZs.

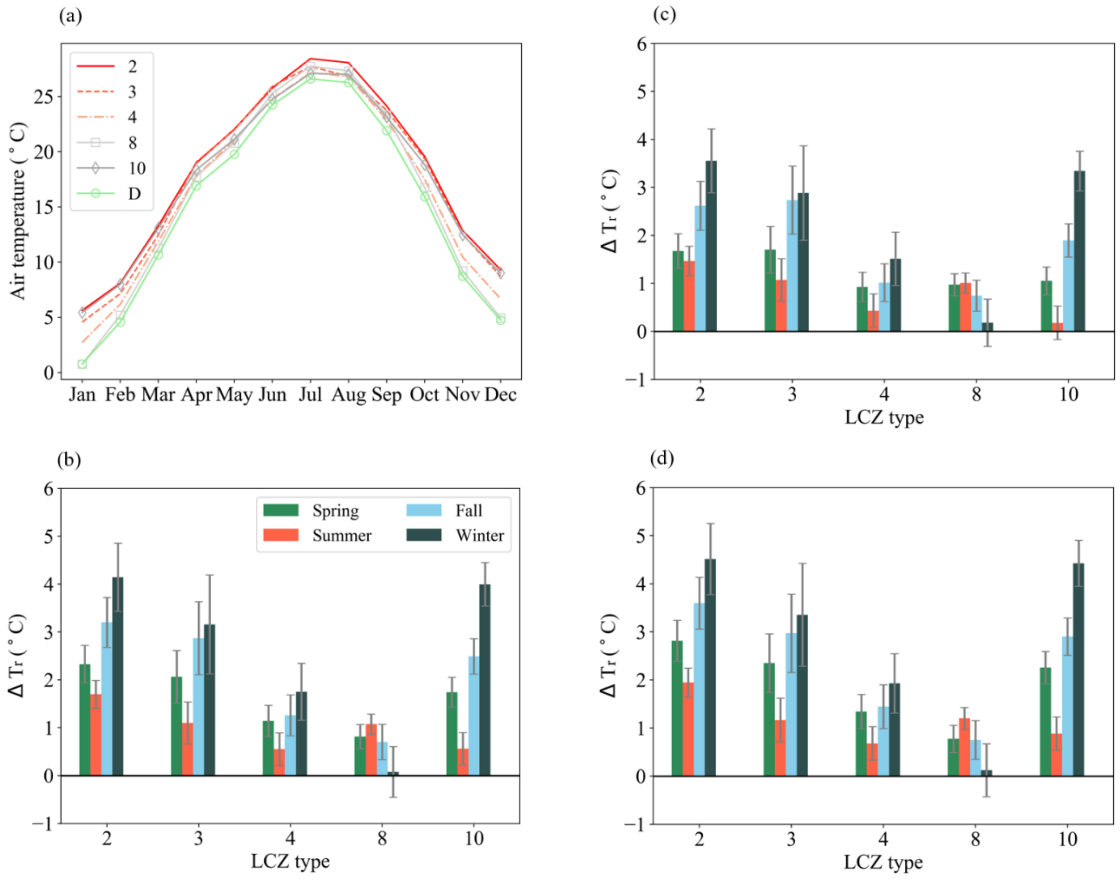

Figure 2. (a) Monthly variation of daily mean temperature over studied LCZ types; Raw (b) daily mean, (c) daytime mean, (d) nighttime mean thermal contrasts (ΔT_r) in four seasons over China. The error bar stands for one standard deviation from the mean of the raw thermal contrast.

3.2 Relation between air temperature and geographical conditions

For each season, one multiple linear regression model is built for daily mean, daytime mean and nighttime mean temperatures, respectively. Figure 3 shows the relations between geographical conditions and average daily mean temperature in fall over studied stations. Air temperatures are found to be negatively correlated with latitude, altitude, and the distance to coastline. Predicted daily mean temperatures are compared against observations in Fig. 3d. It is clear that the linear regression model captures the observed air temperatures in fall reasonably well with a R^2 value of 0.95. Information of the regression models for all seasons is summarized in Table 1. In summer, fall, and winter, R^2 values are greater than 0.9 for all temperatures with RMSEs less than 1.5 ℃, indicating the capacity of built regression models in reproducing the relations between background mean temperature and geographical conditions. Note that the regression coefficients for latitude, altitude and the distance to coastline have considerable seasonal variations. Daily mean temperature reduces about 1 °C per degree latitude in winter, but reduces only about 0.1 °C per degree latitude in summer. Daytime mean air temperature tends to decrease with the distance to coastline in fall but will increase with the distance in other seasons. Though we did not explicitly include meteorological variables in the regression analysis, the seasonal variation of regression models implicitly contained the impact of inter-season change in meteorological conditions on background mean temperature.

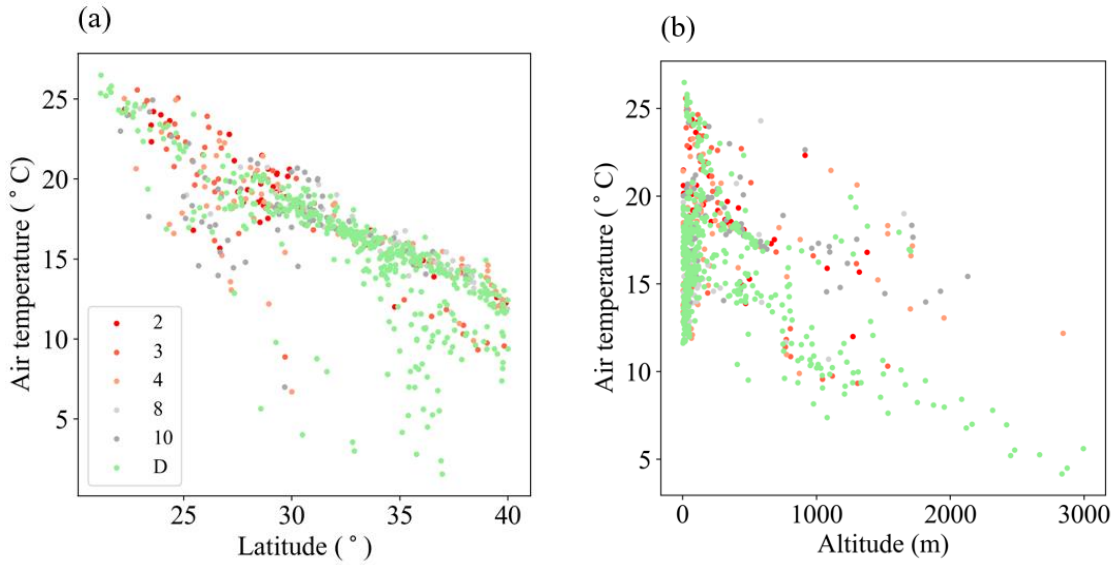

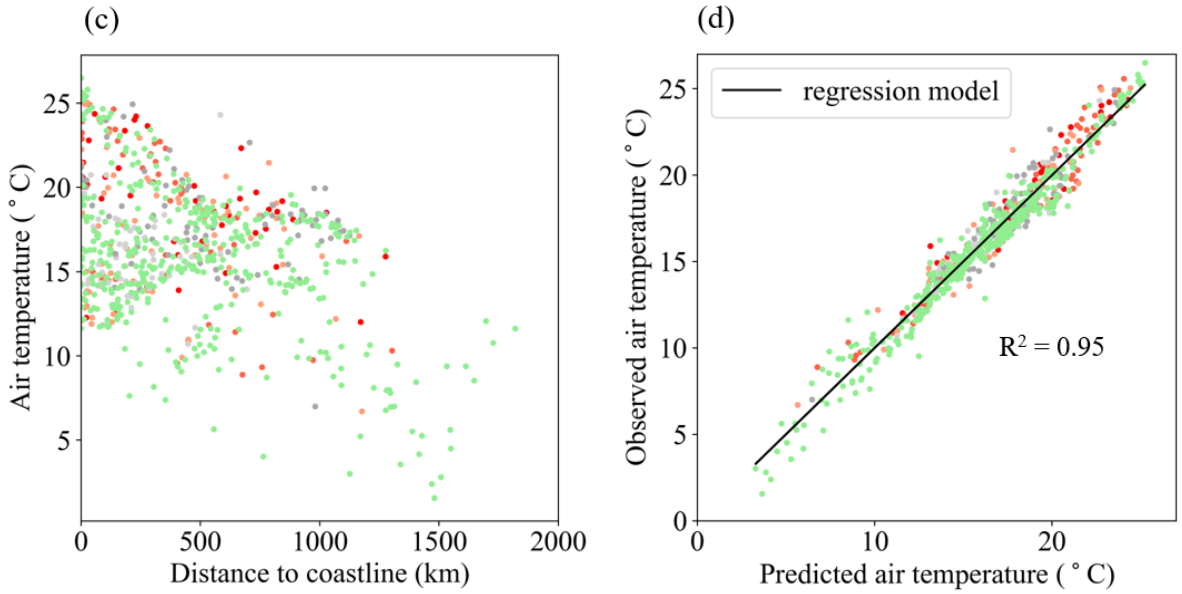

Figure 3. Relationship between (a) latitude, (b) altitude, (c) distance to the coastline and daily mean temperature in fall; (d) comparison of predicted daily mean temperature against observations in fall.

Table 1. Summary of regression models for daily mean, daytime (0900 – 1500 local time) mean, and nighttime (2100 – 0300 local time) mean temperatures in four seasons.

Daily mean temperature					
	LAT coefficient (℃/degree)	ALT coefficient (℃/km)	DCL coefficient (℃/km)	R^2	Root mean square error (℃)
Spring	-0.45	-3.30	1.27×10^{-3}	0.81	1.35
Summer	-0.19	-4.44	1.59×10^{-3}	0.93	0.73
Fall	-0.68	-3.42	-0.07×10^{-3}	0.95	0.89
Winter	-1.02	-3.05	1.26×10^{-3}	0.95	1.20
Daytime mean temperature					
	LAT coefficient (℃/degree)	ALT coefficient (℃/km)	DCL coefficient (℃/km)	R^2	Root mean square error (℃)
Spring	-0.32	-3.08	0.37×10^{-3}	0.73	1.47
Summer	-0.15	-4.39	1.24×10^{-3}	0.92	0.78
Fall	-0.59	-3.13	-0.90×10^{-3}	0.94	0.92
Winter	-0.92	-2.94	0.39×10^{-3}	0.94	1.18

Nighttime mean temperature					
	LAT coefficient (℃/degree)	ALT coefficient (℃/km)	DCL coefficient (℃/km)	R^2	Root mean square error (℃)
Spring	-0.54	-3.46	1.73×10^{-3}	0.84	1.36
Summer	-0.23	-4.49	1.67×10^{-3}	0.93	0.84
Fall	-0.74	-3.70	0.28×10^{-3}	0.95	0.99
Winter	-1.08	-3.24	1.58×10^{-3}	0.94	1.31

3.3 Standard thermal contrast among LCZs

As ΔT denotes only the impact of local landscape, it can be used to examine whether characteristic temperature regimes of LCZs vary with geographical conditions. Results for nighttime temperature in spring over LCZ 10 (heavy industry) is shown as an illustrative example in Fig. 4. Stations in the heavy industry LCZ can have temperature differences in the range of -2 to 3℃ relative to the background temperature. Despite the large variation, ΔT does not correlate with changes in latitude, altitude and the distance to coastline. Note that the large variation here is consistent with values reported in previous studies at the city scale (Geletič et al., 2016; Skarbit et al., 2017; Yang et al., 2018). Take the study in Nanjing, China as an example, nighttime ΔT were found to vary between 1 - 5 ℃ for LCZ 2 and between -1 - 3 ℃ for LCZ 8.

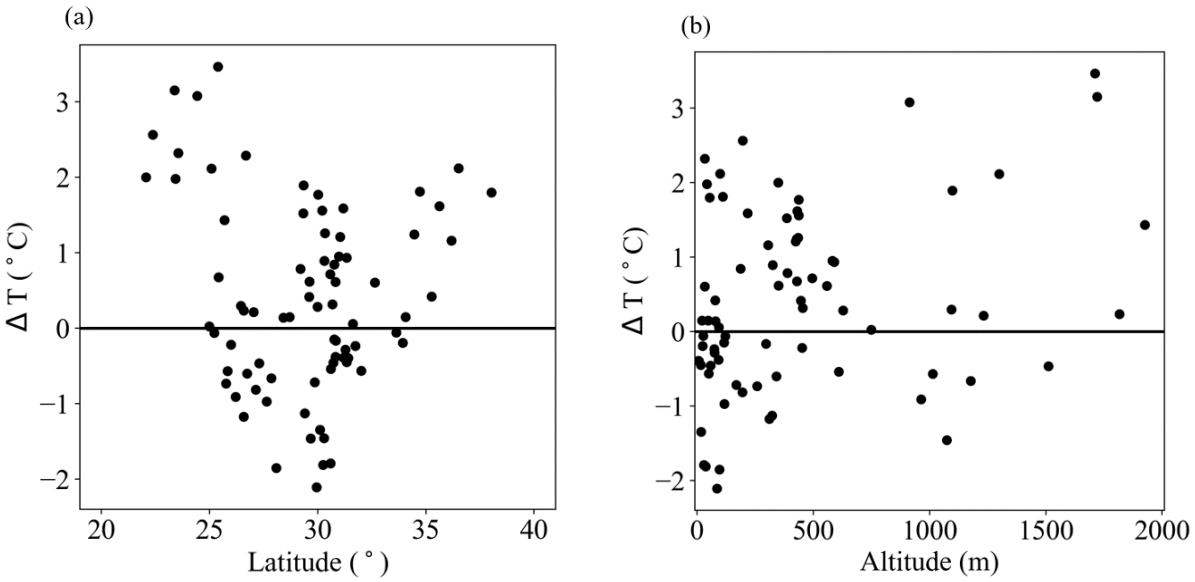

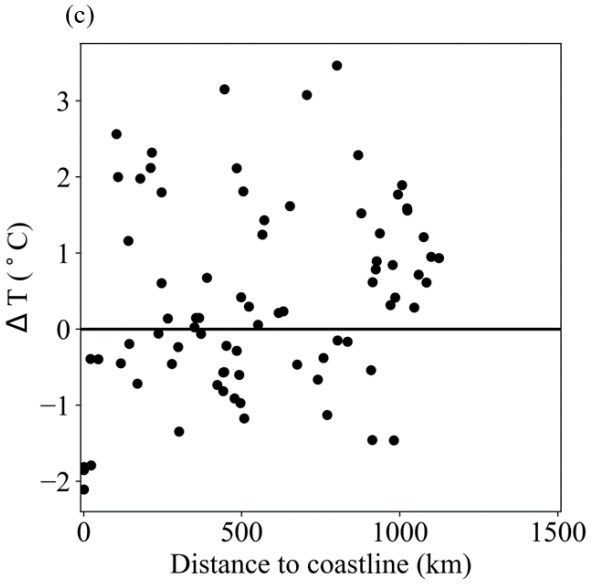

Figure 4. Distribution of the deviation of measured nighttime temperatures from the predicted background temperature (ΔT) over (a) latitude, (b) altitude and (c) distance to coastline over LCZ 10 in spring.

Figure 5 shows the average daily, daytime and nighttime mean ΔT_s in four seasons over China. Compared to Fig. 2, it is clear that standard thermal contrasts are smaller than raw thermal contrasts, with all values below 1 ℃. Annual mean ΔT_s is found to be larger at night (0.51 ± 0.15 ℃, mean ± standard deviation among studied urban LCZs, Fig. 5c) than during daytime (0.22 ± 0.15 ℃, Fig. 5b). For nighttime temperature in winter, the maximum ΔT_s of about 0.8 ℃ is found over LCZ 10 (heavy industry) and the minimum ΔT_s is found over LCZ 3 (compact low-rise). Contrarily, large daytime thermal contrasts are observed over LCZ 3 in summer, while a small negative value occurs over LCZ 10. Daily mean ΔT_s remain relatively constant across four seasons over LCZ 2 (compact mid-rise). Results here clearly demonstrates the different behaviors of characteristic temperature regimes over studied LCZ types in response to seasonal and diurnal variations of meteorological conditions.

We would like to point out that mean variation of ΔT_s within individual LCZs is 0.15 ℃ (error bars in Fig. 5) is as large as the standard deviation of ΔT_s among studied 5 LCZ types. This indicates that when one LCZ has higher mean temperatures than others, some stations belong to that LCZ could have lower temperatures. Such variation is partly due to the structure of the LCZ system, where the ranges of landscape properties used for classifying different LCZs overlap. For example, LCZ 2 and LCZ 3 have the same building surface fraction threshold (40% - 60%) and similar aspect ratio ranges (0.75-2 for LCZ 2 and 0.75-1.5 for LCZ 3). Though many other parameters are involved in the LCZ classification scheme, overlapped ranges inevitably result in large variability in the characteristic temperature regime of LCZs and consequently their thermal contrast.

In spite of the considerable variation, standard thermal contrasts among different LCZs estimated in this study support the validity of the LCZ scheme at the continental scale. Though the magnitudes of standard thermal contrasts are not large, we would like to emphasize that estimated ΔT_s represent the influence on air temperature solely by local urban landscape and do not vary with geographical conditions. Wang et al. (1990) removed the bias related to geographical conditions and reported a mean UHI intensity of 0.23 °C during 1954 – 1983 over entire China. Using observed temperature data in 2016, we find the annual mean air temperature over studied urban LCZs is 0.39 ℃ higher than that over rural areas with low plants. The result indicates that continuous urbanization between 1983 and 2016 has further increased urban-rural temperature difference over China.

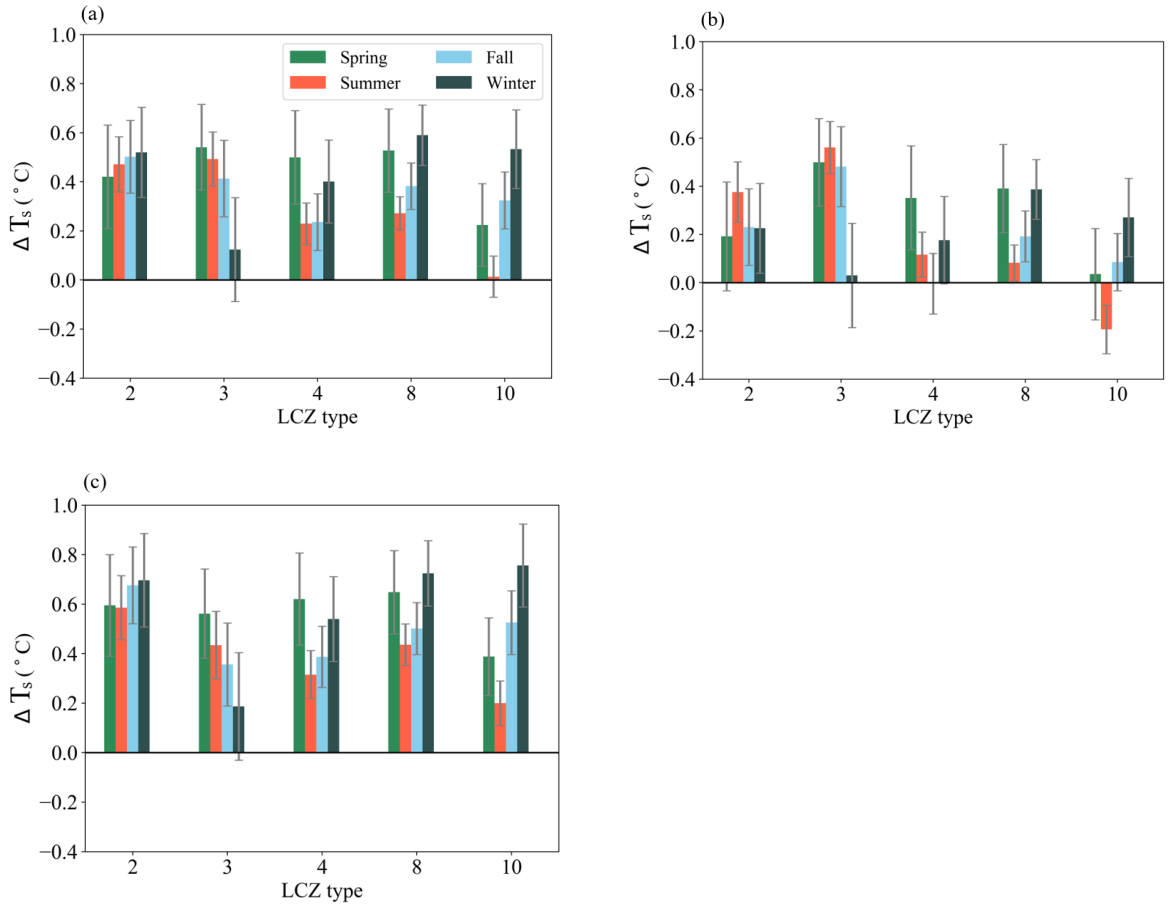

Figure 5. Standard (a) daily mean, (b) daytime mean, (c) nighttime mean thermal contrast (ΔT_s) in four seasons over China. The error bar stands for one standard deviation from the mean of the standard thermal contrast.

4 Conclusions

In this study, we make the first attempt to examine the characteristic temperature regimes of different LCZs across China. Using low plants as the reference LCZ type, raw thermal contrasts directly from station measurements are found to be up to 4 ℃ in winter. After removing the signal of background mean temperature, the standard thermal contrasts become

less than 1 °C for all seasons. Results show that the warmth of urban LCZs is more evident during nighttime, with the maximum effect observed in compact mid-rise zones. The impact of local urban landscape on air temperature over studied LCZ types are consistent at the continental scale and do not change with geographical conditions. Estimated standard thermal contrasts in this study are generalizable for microclimate in other Chinese cities. Large standard thermal contrast with low variations suggests consistently high air temperatures in compact mid-rise neighborhoods (LCZ 2) throughout the year. On the other hand, open high-rise neighborhoods (LCZ 4) have large ΔT_s in winter and low ΔT_s in summer, which is desirable in terms of building energy consumption and outdoor thermal comfort. The findings here thus could provide guidance for urban planning.

The reduction in sensor cost and the ease of data communication have allowed us to monitor the urban thermal environment at a much finer resolution. A recent study showed the critical role of intra-urban climate variability on modifying residents' health risk under extreme events (Yang et al., 2019). The LCZ system provides a good standard for classifying urban neighborhoods with heterogeneous landscape, and facilitates the design and development of urban monitoring networks. Due to data availability, our analysis only focuses on air temperature. Future studies shall investigate the characteristic regime of other variables over different LCZs, such as air humidity and wind speed. Another limitation of this study is the neglect of meteorological conditions in the estimation of standard thermal contrasts. The relation between temperature variability and meteorological conditions in different LCZs is worth further investigation.

Acknowledgments, Samples, and Data

This work was supported by the Hong Kong Research Grants Council funded project 16204220. Due to data policy in China, original hourly temperature data at 2739 stations are not available via a public repository. Anyone of interest could contact China Meteorological Administration (http://www.cma.gov.cn/en2014/) for detailed information of data acquisition. Seasonal daily, daytime and nighttime mean air temperature data in this study is available at: https://doi.org/10.5281/zenodo.3940212. The study of LCZ data development was partially supported by the Vice-Chancellor's One-off Discretionary Fund of The Chinese University of Hong Kong.

References

Alexander, P. J., & Mills, G. (2014). Local climate classification and Dublin's urban heat island. *Atmosphere, 5*(4), 755-774. doi: 10.3390/atmos5040755

Barreca, A., Clay, K., Deschenes, O., Greenstone, M., & Shapiro, J. S. (2016). Adapting to climate change: The remarkable decline in the US temperature-mortality relationship over the twentieth century. *Journal of Political Economy, 124*(1), 105-159. doi: 10.1086/684582

Bechtel, B., Demuzere, M., Mills, G., Zhan, W., Sismanidis, P., Small, C., & Voogt, J. (2019). SUHI analysis using local climate Zones—A comparison of 50 cities. *Urban Climate, 28*, 100451. doi: 10.1016/j.uclim.2019.01.005

Cai, M., Ren, C., Xu, Y., Lau, K. K., & Wang, R. (2018). Investigating the relationship between local climate zone and land surface temperature using an improved WUDAPT methodology–A

case study of Yangtze river delta, China. *Urban Climate, 24*, 485-502. doi: 10.1016/j.uclim.2017.05.010

Chen, X., & Jeong, S. J. (2018). Shifting the urban heat island clock in a megacity: a case study of Hong Kong. *Environmental Research Letters*, *13*(1), 014014. doi: 10.1088/1748-9326/aa95fb

Fenner, D., Meier, F., Bechtel, B., Otto, M., & Scherer, D. (2017). Intra and inter local climate zone variability of air temperature as observed by crowdsourced citizen weather stations in berlin, Germany. *Meteorologische Zeitschrift, 26*, 525-547. doi: 10.1127/metz/2017/0861

Geletič, J., Lehnert, M., & Dobrovolný, P. (2016). Land surface temperature differences within local climate zones, based on two central European cities. *Remote Sensing, 8*(10), 788. doi: 10.3390/rs8100788

Kotharkar, R., & Bagade, A. (2018). Evaluating urban heat island in the critical local climate zones of an Indian city. *Landscape and Urban Planning, 169*, 92-104. doi: 10.1016/j.landurbplan.2017.08.009

Levermore, G., Parkinson, J., Lee, K., Laycock, P., & Lindley, S. (2018). The increasing trend of the urban heat island intensity. *Urban Climate, 24*, 360-368. doi: 10.1016/j.uclim.2017.02.004

Geerts, B., & Linacre, E. (1997). *Climates and weather explained*. Abingdon, Routledge.

Martilli, A., Krayenhoff, E. S., & Nazarian, N. (2020). Is the urban heat island intensity relevant for heat mitigation studies? *Urban Climate, 31*, 100541. doi: 10.1016/j.uclim.2019.100541

Oke, T. R. (1982). The energetic basis of the urban heat island. *Quarterly Journal of the Royal Meteorological Society, 108*(455), 1-24. doi: 10.1002/qj.49710845502

Ramamurthy, P., González, J., Ortiz, L., Arend, M., & Moshary, F. (2017). Impact of heatwave on a megacity: an observational analysis of New York City during July 2016. *Environmental Research Letters*, *12*(5), 054011. doi: 10.1088/1748-9326/aa6e59

Santamouris, M., Cartalis, C., Synnefa, A., & Kolokotsa, D. (2015). On the impact of urban heat island and global warming on the power demand and electricity consumption of buildings—A review. *Energy and Buildings, 98*, 119-124. doi: 10.1016/j.enbuild.2014.09.052

Shi, Y., Lau, K. K., Ren, C., & Ng, E. (2018). Evaluating the local climate zone classification in high-density heterogeneous urban environment using mobile measurement. *Urban Climate, 25*, 167-186. doi: 10.1016/j.uclim.2018.07.001

Skarbit, N., Stewart, I. D., Unger, J., & Gál, T. (2017). Employing an urban meteorological network to monitor air temperature conditions in the 'local climate zones' of Szeged, Hungary. *International Journal of Climatology, 37*, 582-596. doi: 10.1002/joc.5023

Stewart, I. D., Oke, T. R., & Krayenhoff, E. S. (2014). Evaluation of the 'local climate zone'scheme using temperature observations and model simulations. *International Journal of Climatology, 34*(4), 1062-1080. doi: 10.1002/joc.3746

Stewart, I. D., & Oke, T. R. (2012). Local climate zones for urban temperature studies. *Bulletin of the American Meteorological Society, 93*(12), 1879-1900. doi: 10.1175/BAMS-D-11-00019.1

Tomlinson, C. J., Chapman, L., Thornes, J. E., & Baker, C. J. (2011). Including the urban heat island in spatial heat health risk assessment strategies: A case study for Birmingham, UK. *International Journal of Health Geographics, 10*(1), 42. doi: 10.1186/1476-072X-10-42

Verdonck, M., Demuzere, M., Hooyberghs, H., Beck, C., Cyrys, J., Schneider, A., . . . Van Coillie, F. (2018). The potential of local climate zones maps as a heat stress assessment tool, supported by simulated air temperature data. *Landscape and Urban Planning, 178*, 183-197. doi: 10.1016/j.landurbplan.2018.06.004

Wang, C., Middel, A., Myint, S. W., Kaplan, S., Brazel, A. J., & Lukasczyk, J. (2018). Assessing local climate zones in arid cities: The case of Phoenix, Arizona and Las Vegas, Nevada. *ISPRS Journal of Photogrammetry and Remote Sensing, 141*, 59-71. doi: 10.1016/j.isprsjprs.2018.04.009

Wang, W., Zeng, Z., & Karl, T. R. (1990). Urban heat islands in China. *Geophysical Research Letters, 17*(13), 2377-2380 doi: 10.1029/GL017i013p02377

Wienert, U., & Kuttler, W. (2005). The dependence of the urban heat island intensity on latitude–a statistical approach. *Meteorologische Zeitschrift, 14*(5), 677-686. doi: 10.1127/0941-2948/2005/0069

Yang, J., & Bou-Zeid, E. (2019). Designing sensor networks to resolve spatio-temporal urban temperature variations: fixed, mobile or hybrid?. *Environmental Research Letters, 14*(7), 074022. doi: 10.1088/1748-9326/ab25f8

Yang, J., Hu, L., & Wang, C. (2019). Population dynamics modify urban residents' exposure to extreme temperatures across the United States. *Science advances, 5*(12), eaay3452. doi: 10.1126/sciadv.aay3452

Yang, X., Yao, L., Jin, T., Peng, L. L., Jiang, Z., Hu, Z., & Ye, Y. (2018). Assessing the thermal behavior of different local climate zones in the Nanjing metropolis, China. *Building and Environment, 137*, 171-184. doi: 10.1016/j.buildenv.2018.04.009

Zheng, Y., Ren, C., Xu, Y., Wang, R., Ho, J., Lau, K., & Ng, E. (2018). GIS-based mapping of local climate zone in the high-density city of Hong Kong. *Urban Climate, 24*, 419-448. doi: 10.1016/j.uclim.2017.05.008

Zhou, B., Rybski, D., & Kropp, J. P. (2017). The role of city size and urban form in the surface urban heat island. *Scientific reports, 7*(1), 1-9. doi: 10.1038/s41598-017-04242-2

Zhou, D., Zhao, S., Liu, S., Zhang, L., & Zhu, C. (2014). Surface urban heat island in China's 32 major cities: Spatial patterns and drivers. *Remote Sensing of Environment*, *152*, 51-61. doi: 10.1016/j.rse.2014.05.017